

Event trigger generator for resonant spherical detectors of gravitational waves

Stefano Foffa and Riccardo Sturani

Département de Physique Théorique, Université de Genève, Geneva, Switzerland

stefano.foffa, riccardo.sturani@unige.ch

We have set up and tested a pipeline for processing the data from a spherical gravitational wave detector with six transducers. The algorithm exploits the multi-channel capability of the system and provides a list of candidate events with their arrival direction. The analysis starts with the conversion of the six detector outputs into the scalar and the five quadrupolar modes of the sphere, which are proportional to the corresponding gravitational wave spherical components. Event triggers are then generated by an adaptation of the WaveBurst algorithm. Event validation and direction reconstruction are made by cross-checking two methods of different inspiration: geometrical (lowest eigenvalue) and probabilistic (maximum likelihood). The combination of the two methods is able to keep substantially unaltered the efficiency and can reduce drastically the detections of fake events (to less than ten per cent). We show a quantitative test of these ideas by simulating the operation of the resonant spherical detector miniGRAIL, whose planned sensitivity in its frequency band (few hundred Hertz's around 3kHz) is comparable with the present LIGO one.

PACS numbers: 04.80.Nn,95.55.Ym

I. INTRODUCTION

What makes a resonant spherical detector [1, 2] really different from bars [3] and interferometers [4] is the fact of being a multichannel detector. As result, a sphere has almost isotropic sensitivity and enables to reconstruct the gravitational wave (GW) direction. After the seminal work of Wagoner and Paik [5], where the basic features of the detector have been pointed out, more and more detailed sphere models and configurations have been studied by several authors [6, 7, 8, 9, 10, 11, 12, 13, 14]. In particular, various solutions have been proposed to the problems of the ideal transducers configuration [12], parameters reconstruction

[6, 11], and multidimensional data analysis [9].

The analysis method that we have set up and studied in the present work is the result of a synthesis and a refinement of some of these contributions, and is intended to represent the core of the pipeline that we are building for the miniGRAIL detector. MiniGRAIL is one of the two small prototypes of resonant spherical detectors which will be soon operating in the 3kHz region, with the possibility of detecting quasi-normal modes of strange core neutron stars [15] or burst from sub-solar mass black hole coalescences [16].

A greater variety of sources could be studied by building a larger sphere operating in the sub-kHz region and our method, being completely general, could be applied to such detectors as well.

Sec. II of the paper is devoted to building an accurate detector model and to the generation of a simulated set of data. We concentrate on the case of six transducers placed in a specific configuration (the so-called TIGA [10]), which best preserves the spherical symmetry of the detector, and has been adopted by the miniGRAIL team.

For the same reason as above, the parameters of the numerical sphere model (mass, radius, Poisson's ratio, modes and transducers frequencies, temperature, quality factors, readout electronic components) have been chosen in order to mimic the features of miniGRAIL, including asymmetries and possible "imperfections".

We work out the spectrum of each transducer's output and we generate simulated data starting from the elementary noises which are involved at different stages in the detector. Then, we discuss the problem of extracting the GW parameters out of the data.

In sec. III we describe the method to generate trigger of events. We used WaveBurst, the event trigger generator used by the Burst working group of the LIGO-VIRGO joint collaboration, suitably adapted for our multi-mode analysis. Once an event trigger is obtained, the five quadrupolar modes provide a redundant description of a GW signal, which depends on four parameters (the amplitudes of the two polarizations and the two angles identifying the source direction). We exploit this redundancy to distinguish true GW signals from other non-Gaussian noise (like glitches, for instance). The multimode analysis is then able to compute all the relevant quantities of a GW and to reduce the false alarm rate.

Sec. IV contains some results of the analysis, showing the level of signal-to-noise ratio required to obtain the desired accuracy in the direction reconstruction and efficiency.

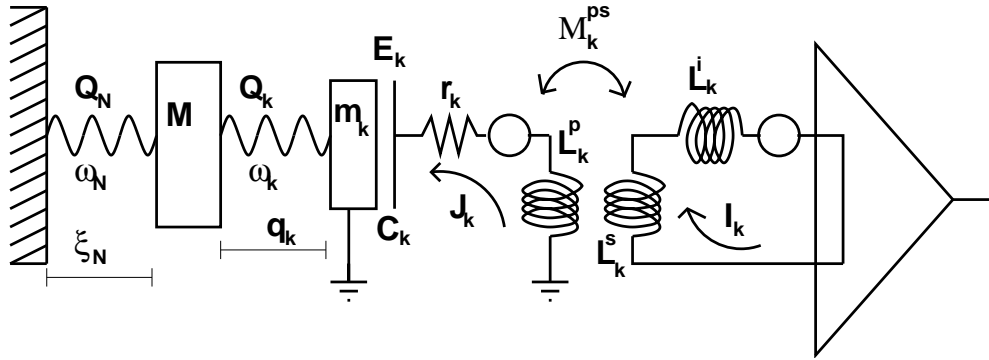


Figure 1: The readout scheme of one of the transducers. The surface of the sphere is modeled as an oscillating mass M , whose displacement is amplified by the six transducers of mass m_k , $k = 1..6$, placed at different positions on the sphere. For each transducer an electric circuit (primary) converts the mechanical displacement into a current I_k which is then converted into a larger current I_k in the secondary circuit. A SQUID finally amplifies the secondary current.

II. MODELING THE DETECTOR

A. Equations for modes, transducers and readout currents

The sphere is well modeled [10, 14] as a set of coupled mechanical and electric oscillators, describing the dynamics of the relevant sphere vibrational modes, of the transducers, and of the electrical circuit that are at the core of the readout devices, see fig. 1.

As the relevant equations have been already discussed in detail by several authors (see for instance the references above), we jump to the mathematical core of the problem, skipping introductory material and definitions that can be found in the literature.

In Fourier space, the detector is described by a system of linear and algebraic equations

$$\{\xi_N, q_k, J_k, I_k\} = \mathcal{Z} \left[f_N, f_k^t, f_k^p, f_k^s, f_k^I \right], \quad (1)$$

where the ξ_N are the amplitudes of the various radial modes of the sphere, the I_k, J_k are the currents flowing in the k -th transducer electric circuit of the readout, the q_k the positions of the relative mechanical oscillators, and the f 's the stochastic forces related to the various dissipative components of the detector. As to the operator \mathcal{Z} , its exact form can be deduced from the equations contained in [10, 14]: for our purposes, what matters is that this operator can be computed numerically as a function of the detector parameters.

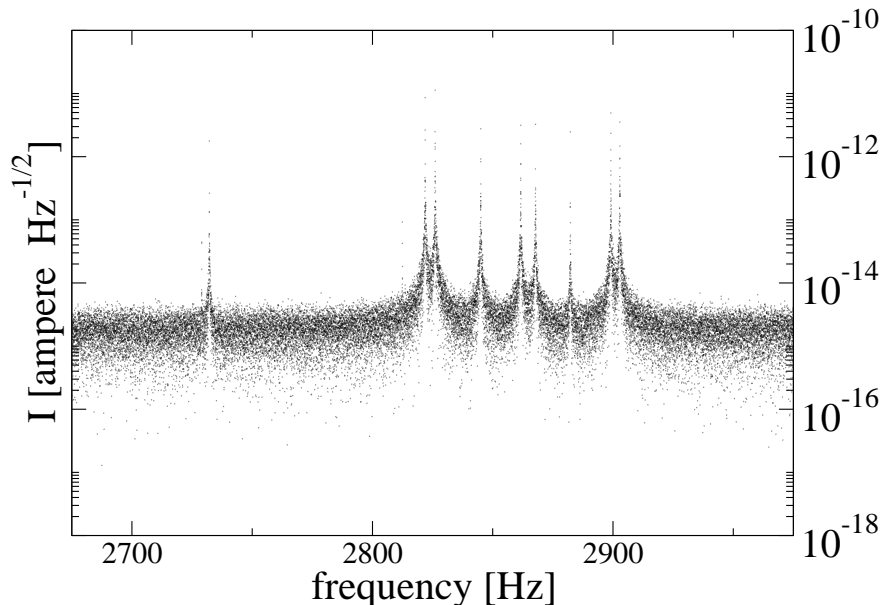


Figure 2: The simulated output of transducer #0.

Since the noise spectral densities of the stochastic forces f 's are known (again, see [10, 14]), a possible detector configuration can be produced thanks to a random number generator; then the corresponding output currents spectral densities can be derived through eq.(1), as shown in figure 2.

B. From currents to the GW wave modes

When a GW impinges the detector, a deterministic force is added to the quadrupolar components of f_N :

$$f_N \rightarrow f_N + \frac{1}{2}R\chi_N\omega^2 h_N \quad \text{for } N = 0, \dots, 4, \quad (2)$$

$$h_{ij} = \sum_{N=0,4} \mathcal{Y}_{m_N,ij}^2 h_N, \quad (3)$$

where R is the sphere radius and $Y_{m_N}^2 = \sum_{i,j} \mathcal{Y}_{m_N,ij}^2 n^i n^j$, being n^i the versor of the arrival direction of the wave and $m_N = 0, 1c, 1s, 2c, 2s$, according to the conventions used in [6].

When six transducers are present, as in the TIGA configuration, the system is in principle overconstrained as the 5 quadrupolar h_M 's are to be determined by the 6 outputs.

In the idealized case, the solution is provided by the *mode channels*, i.e. 5 linear combinations of the currents which are in one to one correspondence with the sphere quadrupolar

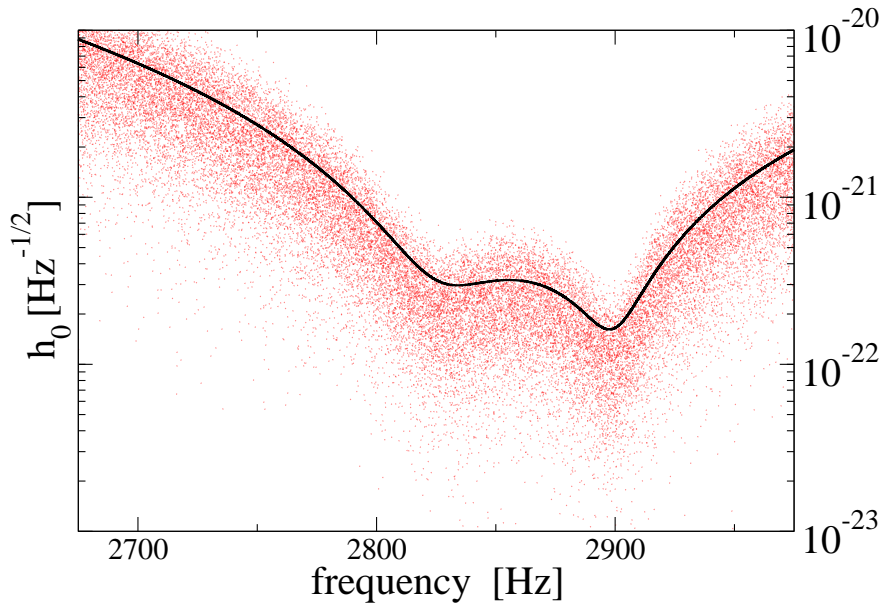


Figure 3: The mode h_0 as it has been reconstructed starting from an actual noise realization, superimposed with its expectation value.

modes [10], while the sixth, remaining combination is insensitive to any such modes.

In the presence of noise and of asymmetries however the exact definition of mode channels is not trivial and require the addition of a sixth vibrational mode of the sphere in the problem, in order to make the system invertible [18].

We chose then to include the scalar mode in the system, as this is the mode that in the idealized case is probed by the sixth linear combination of current outputs. Moreover, the determination of the scalar mode allows, in principle, to test alternative theories of gravity (where scalar GW's can exist), or to build a veto, as events exciting such mode cannot be reduced to Einstein general relativity GW's.

Given these premises, the problem can now be numerically solved (for every value of ω) to give

$$h_N(\omega) = T_{Nk}(\omega) \cdot I_k(\omega), \quad (4)$$

where $T_{Nk}(\omega)$ defines the *transfer function* (which in this case is actually a transfer matrix) of the system.

We can now use eq.(4) to express any realization of the detector output in terms of GW quadrupolar modes, as shown in figure 3. Moreover eq.(4) can be combined with the results

of the previous paragraph in order to give the h_N spectral density matrix:

$$\langle I_k(\omega)I_{k'}^*(\omega') \rangle \rightarrow T_{Nk} \rightarrow \langle h_N(\omega)h_{N'}^*(\omega') \rangle \equiv S_{NN'}^h(\omega)\delta(\omega - \omega'), \quad (5)$$

which can be used to estimate the detector sensitivity.

III. THE ANALYSIS PIPELINE

We have just hinted how to generate six time series corresponding to the quadrupolar plus scalar mode. As at this stage we are not interested in the scalar GW component, then we will restrict the analysis to the five quadrupolar modes, which will be enough and necessary to reconstruct the most general *symmetric, traceless* 3×3 matrix.

Still this is a redundant description of a GW, and we will exploit this redundancy to discriminate between real GW signals and excitations of the modes due to disturbances other than gravitational.

A. The scalar trigger

If one knew exactly the form of the expected signal, the optimal strategy would be to perform a multidimensional matched filtering, but we would like to find triggers out of the stretch of data, without any need of a detailed knowledge of the signal. This can be done by building the following quantity:

$$H(\omega) = (h \cdot h)_S, \quad (6)$$

which is a generalization of the one proposed in [13], and takes account of the differences and of the correlations among the various quadrupolar modes, as the r.h.s. is defined by

$$(X \cdot Y)_S \equiv \sum_{N, N'=0\dots 4} X_N^\dagger(\omega)(S_{NN'}^h)^{-1}(\omega)Y_{N'}(\omega). \quad (7)$$

The Fourier transform of this quantity is then fed to a suitably adapted version of WaveBurst, one of the burst event trigger generators used in the LIGO data analysis [19, 20]. The WaveBurst algorithm make use of the wavelet decomposition, and among the bank of wavelet packets we picked the Symlet base with filter length sixty [24]. Using an orthogonal wavelet transformation the time series are converted into wavelet series W_{ij} where i is the time

index and j the wavelet *layer* index. Each wavelet layer can be associated with a certain frequency band of the initial time series. The time frequency resolution varies according to the *decomposition level*, if \mathcal{N} is the number of data in the initial time series, at decomposition level n the number of layers is 2^n , each with $\mathcal{N} \times 2^{-n}$ points (the procedure can go on as long as $\mathcal{N}2^{-n}$ is an integer).

For each layer a fixed fraction of the coefficients W'_{ij} s with the largest absolute magnitude is selected and WaveBurst keeps as triggers only those coefficients whose selection is robust under change of the decomposition level. Each trigger consists of highlighting a connected region in the time-frequency plane where the wavelet coefficients exceed an adaptive threshold (e.g. the 0.5% higher coefficients).

An eventual GW signal impinging on the detector will have different strength in different channels, depending on the arrival direction and polarization, whereas in H , see eq.(6), it will imprint almost exactly the same signal, no matter its polarization nor arrival direction.

Once the trigger has been established the analysis is performed on the modes h_N 's, by collecting the values of the wavelet coefficients for each channel and for each trigger. At this point we can try to reconstruct the arrival direction in (at least) two different ways.

As a first method one hand one can find the values of θ, ϕ which maximize the *a posteriori* probability of having our stretch of data given that a GW hit the detector see sec.III B. However this method will give a determination of the would be GW direction no matter if a real GW has excited the detector or a glitch, say, or any other noise excitation not compatible with a transverse, traceless GW event has taken place. To confirm this direction determination we combine it with a different, geometric method, see sec. III C. When the two methods do not determine the same directions, within some tolerance to be discussed quantitatively in sec. IV, the event can be discarded as spurious.

B. Likelihood method for direction reconstruction

The posterior probability of having a given stretch of data $\{h_N\}$ assuming a GW with polarization strength h_+ and h_\times from the direction identified by the usual polar angles θ, ϕ is denoted by $p(\{h_N\}|h_+, h_\times, \theta, \phi)$. The N mode response to the gravity wave is

$$\xi_N = F_N^+(\theta, \phi)h_+ + F_N^\times(\theta, \phi)h_\times, \quad (8)$$

where $F_N^{+,\times}$ is the pattern function of the N mode for the $+, \times$ polarization.

Following the standard procedure [21, 22], the following likelihood ratio can be defined

$$\Lambda = \frac{p(\{h_N\}|H_{\xi_N})}{p(\{h_N\}|H_0)}, \quad (9)$$

where the H_{ξ_N} is the hypothesis that a GW characterized by ξ_N is present in the data and H_0 is the hypothesis that no GW is in the data.

For stationary, Gaussian, white noise with zero mean, and by taking into account that the noises in the different channels are correlated, the above mentioned probability densities are

$$\begin{aligned} p(\{h_N\}|H_{\xi_N}) &\propto \exp[-((h - \xi) \cdot (h - \xi))_S/2], \\ p(\{h_N\}|H_0) &\propto \exp[-(h \cdot h)_S/2], \end{aligned} \quad (10)$$

and the logarithm of the likelihood ratio can then be expressed as

$$\mathcal{L} = \ln(\Lambda) = \mathcal{R}e[(\xi \cdot h)_S] - \frac{1}{2}(\xi \cdot \xi)_S. \quad (11)$$

By maximizing eq. (11) with respect to h_+, h_\times a function $L(\theta, \phi)$ of the angles alone is found

$$\begin{aligned} L(\theta, \phi) &= \frac{1}{2} \left[(F^+ \cdot F^+)_S (F^\times \cdot F^\times)_S - (F^+ \cdot F^\times)_S^2 \right]^{-1} \times \\ &\left[(F^\times \cdot F^\times)_S (h \cdot F^+)_S^2 + (F^+ \cdot F^+)_S (h \cdot F^\times)_S^2 - 2(h \cdot F^+)_S (h \cdot F^\times)_S (F^+ \cdot F^\times)_S \right] \end{aligned} \quad (12)$$

The values of θ, ϕ (which enter the expression for the F_N 's) maximizing $\sum_{\{trigger\}} L(\theta, \phi)$, that is the sum of the likelihood over every point of time-frequency plane exceeding the threshold, give the arrival direction of the candidate event.

C. Geometric method for direction reconstruction

Another method to reconstruct the direction of arrival of the GW by exploiting the (redundancy of the) five quadrupolar modes is based on linear algebra considerations [10]. A general metric perturbation h_{ij} (the temporal components are suppressed here) representing a GW coming from the z axis can be written as

$$h_{ij} = \begin{pmatrix} h_+ & h_\times & 0 \\ h_\times & -h_+ & 0 \\ 0 & 0 & 0 \end{pmatrix}. \quad (13)$$

For a different incoming direction the specific shape of the metric perturbation will be different, but the *eigenvalues* of the matrices will be the same, thus implying that a generic GW is always represented by a *traceless* matrix with a *zero eigenvalue* (thus implying that the non zero eigenvalues are equal in magnitude and opposite in sign). In particular the direction of the zero eigenvalue is the propagation direction of the GW. Of course none of the eigenvalues is expected to be exactly zero at every instant within the duration of the trigger, so for each instant of time the direction of the smallest absolute magnitude eigenvalue is computed. We then weight each direction with an empirical factor $1/r$, taking into account how the eigenvalues are close to the ideal, noiseless situation described by (13).

After ordering the three eigenvalues λ_i so that $|\lambda_0| \leq |\lambda_1| \leq |\lambda_2|$ we define the following quantities

$$r \equiv \frac{\sqrt{2}|\lambda_0|}{\sqrt{\lambda_1^2 + \lambda_2^2}}. \quad (14)$$

For a perfect GW like (13) r vanishes, thus the smallest it is, the less the noise is contaminating the GW signal.

IV. RESULTS

To check our method we injected in software both GW signals and signals exciting of equal strength on the different channels, corresponding to a metric perturbation of the type

$$h_{ij} = \begin{pmatrix} (\sqrt{3}-1)/\sqrt{3} & 1 & 1 \\ 1 & -(\sqrt{3}+1)/\sqrt{3} & 1 \\ 1 & 1 & 2/\sqrt{3} \end{pmatrix}, \quad (15)$$

which is incompatible with a GW. We investigated how well we could recover the injections of both real and fake signals in each of the channels with different waveforms.

We injected sine-gaussian with a time-width of 50msec, central frequency $2825Hz$ and with $h_{rss} = 10^{-20}Hz^{-1/2}$, see fig. 4. Fig. 5 refers to an injection of 25 polarized GW-signals incoming from the direction specified by the angle $\theta = 55^\circ$, $\phi = 45^\circ$, whereas fig. 6 refers to a signal of the type described by eq.(15), or fake-injection, with the same shape and strength. The two direction identification methods agree much better in the case of GW rather than in the fake-injection case see fig. 7, where an almost flat distribution of distances is obtained.

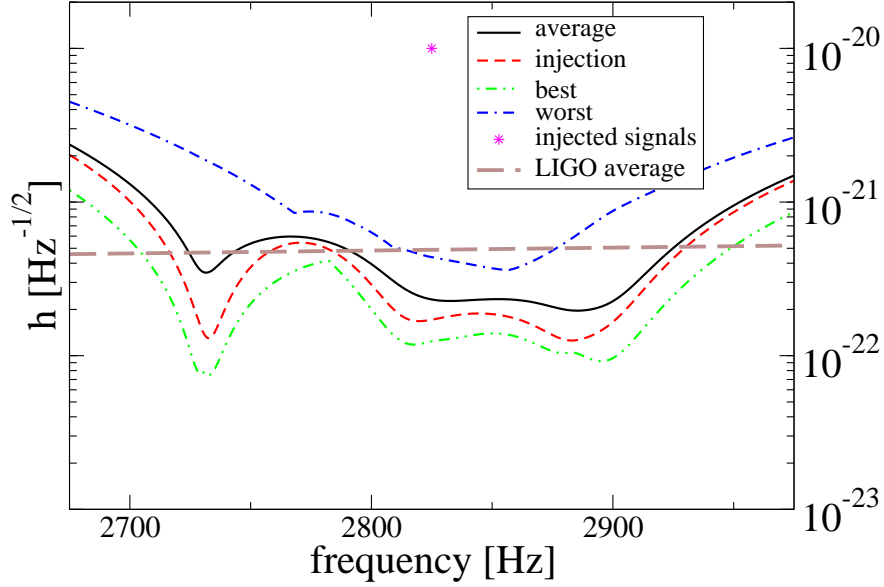


Figure 4: The stars indicate the injections, while the dashed line is the strain sensitivity for the arrival direction of the injections. For comparison, we have displayed also the averaged sensitivity (continuous line), as well as the ones corresponding, at any given value of the frequency, to the best and worst possible directions. Finally, the thick dashed line is the LIGO current averaged on the sky.

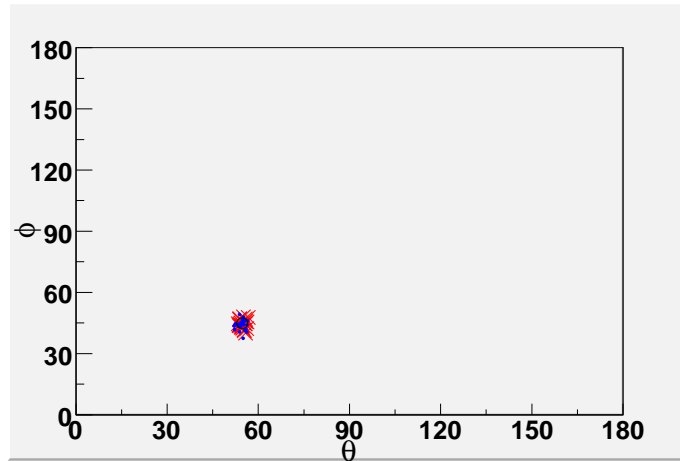


Figure 5: The dots indicate direction reconstruction through the “determinant” method, the crosses through the likelihood one. The injection direction is marked by a circle. Both dots and crosses fall very well on the top of the injection direction.

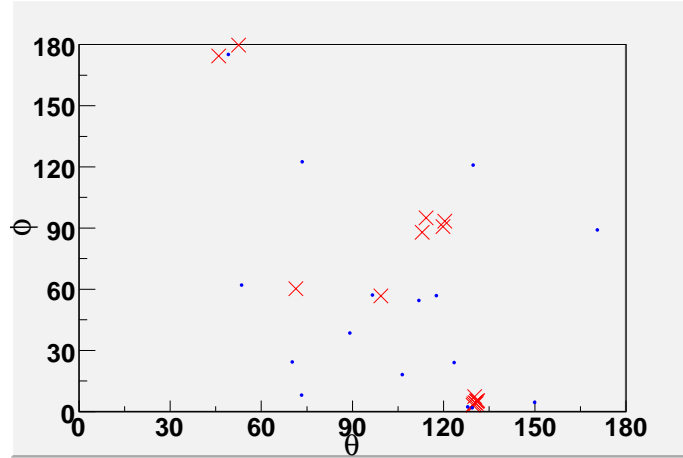


Figure 6: The dots indicate direction reconstruction through the “determinant” method, the crosses through the likelihood one. The signal injected does not correspond to a GW.

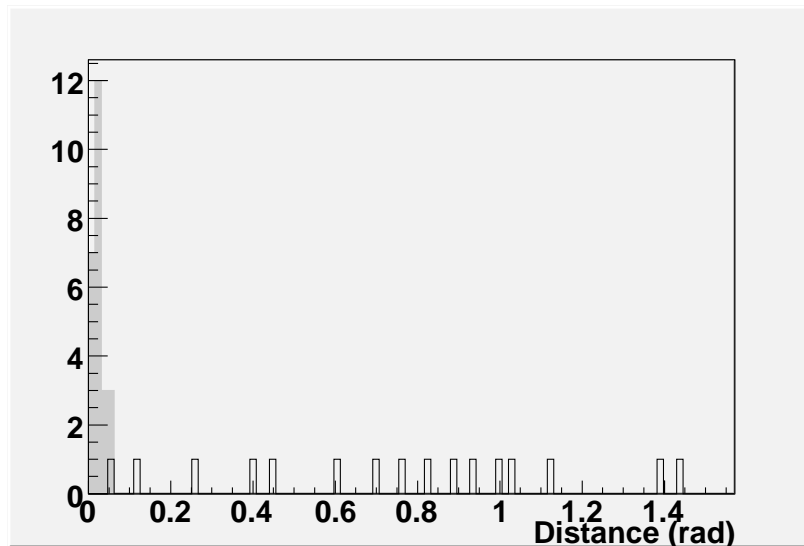


Figure 7: Distribution of angular distances between the directions reconstructed with the two different methods in the case of GW-injections (grey-filled) and fake-injections (black-transparent).

We then propose the combination of these methods can be used to reduce the false alarm rate of a single detector.

Still, from the fig.7 it can be seen that by setting the maximum acceptable distance to 0.1, say, one has perfect efficiency and still picks in some 8% of the non GW-signals, thus suggesting that operating in coincidence with another detector is advisable. Moreover fig. 8 hints that the likelihood method is more efficient than the determinant one in determining the direction. [25]

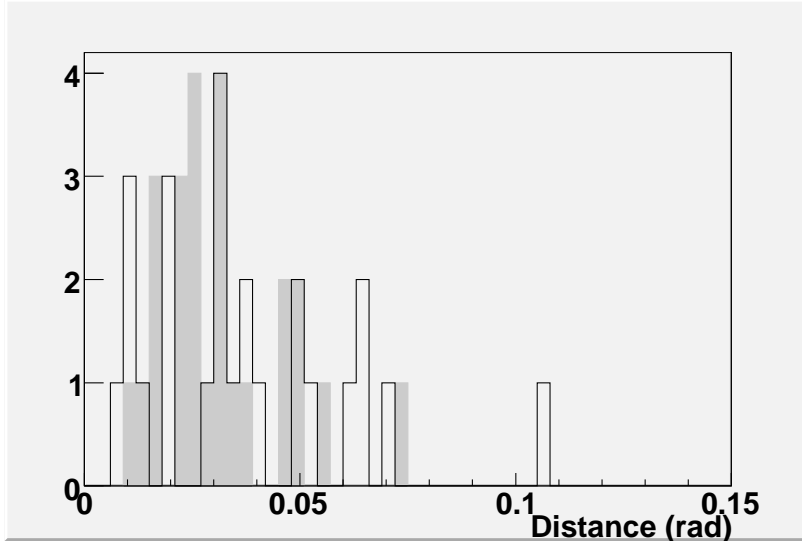


Figure 8: Distribution of angular distances between the injection direction and the directions reconstructed with the likelihood (grey-filled) and with the determinant method (black-transparent) in the case of GW-injections. The average in the two cases is respectively $\mu_l = 0.030$ ($\sigma = 0.015$), $\mu_d = 0.037$ ($\sigma = 0.023$).

We thus conclude these display of preliminary results by claiming that the information a spherical detector can provide can indeed determine the arrival direction of a GW and can discriminate between real GW's and glitches, say, even if more work is needed to make this result more quantitative and solid.

V. CONCLUSION

We have simulated a spherical detector and shown that a resonant sphere detector is capable of detecting the direction of arrival of a gravitational wave. We have shown that at (amplitude) $\text{SNR} \simeq 53$ (corresponding to signals with $h_{rss} = 1 \times 10^{-20} \text{Hz}^{-1/2}$) the likelihood method is well able to determine the direction, but it is not able to discriminate between real GW events and other kind of excitations, as for instance one with all modes excited equally. By cross-checking this method with a different one like we did it is possible to obtain an independent determination of the direction, which leaves substantially unaltered the efficiency and lower the false alarm rate to 8% of the rate of fake events. More work has to be done to assess the method at different at SNR and with higher statistics.

To further lower the false alarm rate it is advisable to work in coincidence, with another sphere, which could give an additional determination of the arrival direction, or with interferometers, which are poor in direction source determination, even if used as a network.

Acknowledgments

The authors acknowledge support from the Boninchi foundation. The authors wishes to thank Giorgio Frossati for his encouragement and support. R.S. wishes to thank the organizers of the GWDAW-12 meeting. During most of the time he has been working at this, R.S. has been supported by an INFN post-doctoral grant. R.S. wishes to thank Gabriele Vedovato and Sergey Klimenko for their help with the WaveBurst algorithm.

References

-
- [1] www.minigrail.nl.
 - [2] O. D. Aguiar *et al.*, *Class. Quant. Grav.* **23** (2006) S239.
 - [3] www.auriga.lnl.infn.it, www.roma1.infn.it/rog.
 - [4] www.ligo.caltech.edu, www.virgo.infn.it, www.geo600.uni-hannover.de, tamago.mtk.nao.ac.jp.
 - [5] R. V. Wagoner and H. J. Paik (1977). In *Experimental Gravitation, Proceedings of the Pavia International Symposium*, Accademia Nazionale dei Lincei, Roma.
 - [6] C. Z. Zhou and P. F. Michelson, *Phys. Rev. D* **51** (1995) 2517.
 - [7] E. Coccia, J. A. Lobo and J. A. Ortega, *Phys. Rev. D* **52**, 3735 (1995).
 - [8] J. A. Lobo and M. A. Serrano, *Europhys. Lett.* **35**, 253 (1996).
 - [9] T. R. Stevenson, *Phys. Rev. D* **56** (1997) 564.
 - [10] S. M. Merkowitz and W. W. Johnson, *Phys. Rev. D* **56** (1997) 7513 [arXiv:gr-qc/9706062].
 - [11] S. M. Merkowitz, *Phys. Rev. D* **58** (1998) 062002 [arXiv:gr-qc/9712079].
 - [12] J. A. Lobo, *Mon. Not. Roy. Astron. Soc.* **316** (2000) 173 [arXiv:gr-qc/0006109].
 - [13] M. A. Gasparini and F. Dubath, *Phys. Rev. D* **74** (2006), 122003.
 - [14] L. Gottardi, *Phys. Rev. D* **75** (2007), 022002.

- [15] O. Benhar, V. Ferrari, L. Gualtieri and S. Marassi, *Gen. Rel. Grav.* **39** (2007) 1323 [arXiv:astro-ph/0603464].
- [16] T. Nakamura, M. Sasaki, T. Tanaka and K. S. Thorne, *Astrophys. J.* **487** (1997) L139 [arXiv:astro-ph/9708060].
- [17] C. D. Tesche and J. Clarke, *J. Low.Temp. Phys.* **29** (1977) 301; C. D. Tesche and J. Clarke, *J. Low.Temp. Phys.* **37** (1979) 397;
- [18] S. Foffa and R. Sturani, arXiv:0805.0718 [gr-qc].
- [19] S. Klimenko, I. Yakushi, M. Rakhmanov and G. Mitselmakher, 2004 *Class.Quant.Grav.* **21** S1685.
- [20] S. Klimenko and G. Mitselmakher, 2004 *Class.Quant.Grav.* **21** S1819.
- [21] E. E. Flanagan and S. A. Hughes, *Phys. Rev. D* **57** (1998) 4566 [arXiv:gr-qc/9710129].
- [22] W. G. Anderson, P. R. Brady, J. D. E. Creighton and E. E. Flanagan, *Phys. Rev. D* **63** (2001) 042003 [arXiv:gr-qc/0008066].
- [23] S. Klimenko, S. Mohanty, M. Rakhmanov and G. Mitselmakher, *Phys. Rev. D* **72** (2005) 122002 [arXiv:gr-qc/0508068].
- [24] Mallat S. "A wavelet tour in signal processing", Academic Press, 1998, chap. VII.
- [25] If instead the source direction is known, a match-filter can be applied.